Desalination and Water Treatment
www.deswater.com
1944-3994/1944-3986 © 2013 Desalination Publications. All rights reserved
doi: 10.1080/19443994.2012.705052

51 (2013) 1362–1365
February

Taylor & Francis
Taylor & Francis Group

Effect of temperature difference on performance of membrane crystallization-based membrane distillation system

Young-Sun Park[a,b], Chang-Kyu Lee[b], Seog-Ku Kim[b], Hyun-Je Oh[b], Sang-Ho Lee[c], June-Seok Choi[b,*]

[a]*Department of Construction Environment Engineering, University of Science & Technology, Deajeon 305-333, Korea*
[b]*Korea Institute of Construction Technology, Goyang-Si, Gyeonggi-Do 411-712, Korea*
Tel. +82 31 910 0759; Fax: +82 31 910 0790; email: jschoi@kict.re.kr
[c]*Department of Construction and Environmental Engineering, Kookmin University, Seoul 136-702, Korea*

Received 16 March 2012; Accepted 15 June 2012

ABSTRACT

This study explores membrane distillation (MD) is suitable to recover pure water and to generate the supersaturation condition for the crystal formation. The system was carried out under a different temperature of feed solution. It was observed that the increase in the mass flux of product solution is due to the increase in the temperature difference between the feed and product solution. Although the temperature difference is important for the mass flux of product solution, it needs to consider a reasonable temperature difference. The highest rejection (%) was observed at feed temperature 60˚C and it is easy to control. It was found that both surface crystallization and bulk crystallization influenced the flux decline of MD. Calcium sulfate crystals can be produced by MD crystallization with a growing crystal size distribution and average size of 100 μm.

Keywords: Seawater desalination; RO brines; Membrane distillation; Calcium sulfate; Crystallization

1. Introduction

As water resources become more limited, desalination of water containing salt (i.e. seawater, brackish water, and wastewater) is becoming a significant technology [1,2]. Since desalination market is now moving to SWRO, reverse osmosis (RO) market is growing rapidly. There are some problems in the application of RO for desalination. The first one is that RO recovery varies from 35 to 50%, which results in a limitation of the water production capacity [3]. Depending on the RO recovery rate, the volume of RO brines is determined and it must be handled and disposed off properly. RO concentrate contains dissolved and particulate contaminants removed from the feedwater and may contain chemicals from pretreatment facilities [4]. Membrane distillation (MD) is a thermal process, in which only vapor molecules transport through porous hydrophobic membranes. It is one of the promising technologies to resolve water shortage issues. The advantages of MD include (1) lower operating temperatures and vapor space than multistage flash and multieffect distillation, (2) less operating

*Corresponding author.

Presented at the International Conference on Desalination for the Environment, Clean Water and Energy, European Desalination Society, 23–26 April 2012, Barcelona, Spain

pressure than RO, and (3) water recovery process at high solute concentrations [5]. MD is considered as a complementary process for the treatment of RO brines. The brine volume could be reduced by a factor of 5.5, but the brine was concentrated 4.6 times [3]. The idea of this study is to use MD crystallization (MDC) to further concentrate RO brines and propose a high recovery integrated process for SWRO. We studied the performance of membrane crystallization-based MD system to change the temperature of feed solution. This work investigated the effect of operating temperature on MD performance (e.g. flux) with two types of different feedwaters (35 g/L NaCl solution and 2 g/L $CaSO_4$ solution).

2. Experimental

2.1. Membrane distillation

All the experiments were performed with a laboratory-scale MD test unit (Fig. 1). The MD test unit consisted of hydrophobic membrane cell, two pumps (Masterflux®, Cole-parmer), feed and product reservoirs, temperature control system, and data acquisition system. A plate-and-frame membrane module has 2 mm channel height and 8.2 cm wide × 8.2 cm long membrane dimensions. We have used commercially available hydrophobic Polyvinylidene fluoride (PVDF) (Durapore®, Millipore) membranes. The membrane characteristics like pore size, porosity, and thickness are given in Table 1. In this unit, feed solution was held in a 2.0 L reservoir and heated by a thermal bath, Agitator (BW-10H, Jeio Tech). After that, it was pumped through the membrane module. Product solution reservoir was filled with 2.0 L of distilled water, and temperature was controlled by circulating chilled water through a stainless steel coil immersed in the product solution. The transmembrane flux was measured by an installed balance (Explorer, Ohuas) connected to data acquisition system and electric conductivity was measured by a conductivity meter (MultiLine, WTW) for rejection rate (%).

Table 1
Membrane properties

Manufacturer	Material	Porosity (%)	Pore size (μm)	Thickness (μm)	Effective area (m^2)
Millipore (GVHP)	PVDF	75	0.22	125	0.0067

Operating conditions of the laboratory-scale MD test unit are summarized in Table 2. Experiments were performed at different feed temperatures to determine the effect of temperature difference on product solution flux. This schematic description describes MD system only. At first, MD was performed in a single closed mode without the crystallizer to examine performance for reaching the supersaturation condition. The crystallization system will be added for further study.

2.2. Crystal size distribution

We measured the particle size of crystals using a particle size analyser (Mastersizer2000, Malvern). Seven suspension samples were taken, 50 ml each from the feed outlet after passing through the membrane. Turbidity was measured using this sample,

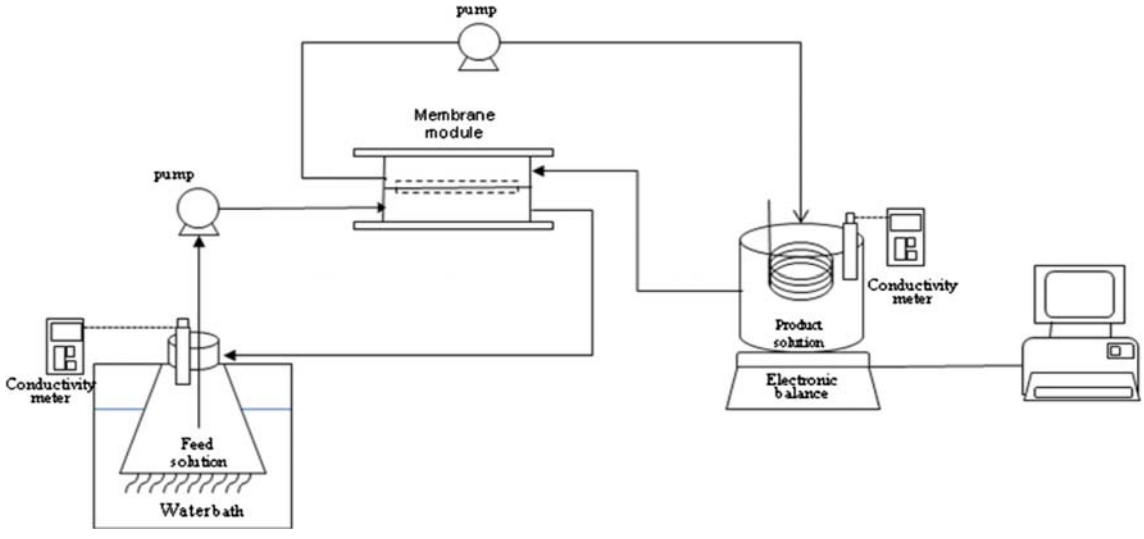

Fig. 1. Schematic description of the MD test unit.

Table 2
Operating conditions of the lab-scale MD test unit

Item		Condition
Solution	Feed side	50, 60, and 70℃
	Product side	Fixed at 20℃
Temperature	Feed	① 35 g/L of NaCl with DI water ② 2 g/L of $CaSO_4$ with DI water
	Product	DI water
Cross-flow velocity	Feed side	0.8 L/min
	Product side	1.0 L/min

after that the crystal size distribution was also measured. The reported batch duration was numbered as starting from the point of supersaturation generated by the MD process.

3. Results and discussion

3.1. Effect of temperature difference on performance of MD

There were product flux variations with the temperature difference (Fig. 2). Since driving force of MD is the vapor pressure difference between both membrane sides, permeate flux is zero when the temperature of feed and product sides are equal. As temperature differences increased from 30 to 50℃, permeate fluxes increased for both the test solutions. This is due to the exponential increase of the vapor pressure of the feed solution with temperature, which increases the transmembrane vapor pressure [6]. When the temperature difference was 50℃ (20/70℃), the highest flux appeared at 15.17 LMH in the synthetic feed solution. Although the highest flux was shown that flux was not constant, because it is difficult to control the high temperature around 70℃. Moreover, the highest rejection (%) calculated from the electric conductivity was observed at 60℃. Therefore, flux decline and crystallization test was performed at fixed temperature difference of 40℃ (20/60℃) in the next chapter.

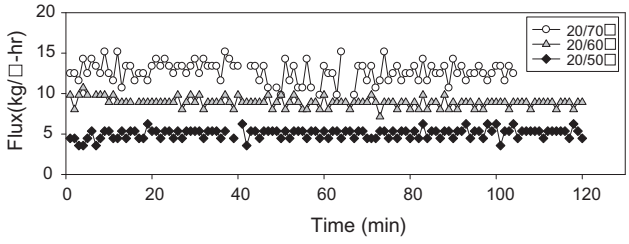

Fig. 2. Effect of temperature difference on permeate flux (35 mg/L of NaCl).

3.2. Flux decline and crystal formation in MD

In this study, MD was operated for concentration of feed solution to reach supersaturation condition. Electric conductivity in feed solution increased continuously with time (Fig. 3).

Fig. 4 illustrates the variation of flux during the MD of calcium sulfate solution as a function of time. The initial flux is 13.25 kg/m^2 h, which is the maximum flux in this test duration. The first period of this result is that, the permeate flux was maintained at initial value during 108 min after that it declined gradually. The significant flux drop was observed after 440 min. The experimental $CaSO_4$ solution has the supersaturation concentration of 2,000 ppm at the beginning. But no flux decline occurred in Step 1, which means that the crystallization needs the induction time to create sufficient nucleus from the supersaturated concentration. Although the concentration of retentate solution was in excess of a critical supersaturation level, the turbidity of the retentate is nearly as

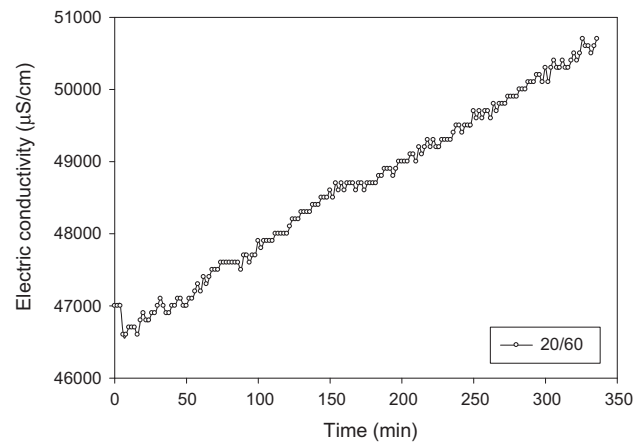

Fig. 3. Electric conductivity incline in feed reservoir.

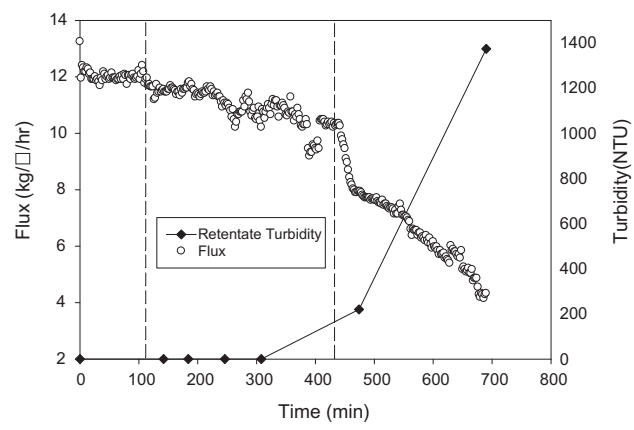

Fig. 4. Flux decline in MD and turbidity.

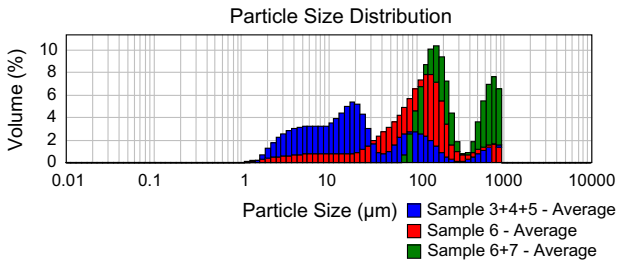

Fig. 5. Particle size distribution of calcium sulfate crystals in retentate sample (2 mg/L of $CaSO_4$).

same as the initial turbidity during Step 2. It means that crystals still did not form in retentate solution. But the surface crystallization resulted in slight decline of flux. In surface blockage mechanism, scale formation may occur due to heterogeneous crystallization on membrane surface and the membrane surface becomes blocked by the lateral growth of crystals [7]. Since most of the crystals formed in retentate through the bulk crystallization, turbidity increased sharply after 440 min. The intensive bulk crystal particle accumulated the cake on the membrane, consequently, the permeate flux declined rapidly.

Observing the crystal growth in bulk solution with time, crystal size distribution of $CaSO_4$ is measured using six samples taken from different duration times. Samples 3–5 were too low concentration to measure crystal size separately. For this reason, the samples were mixed together but it was definitely shown the three of peaks. The first peak appeared between 17.835 and 24.225 μm. The second peak appeared between 91.201 and 158.489 μm. The last peak appeared between 746.3 and 988.5 μm. Sample six was taken right before the formation of bulk crystals. And numerous crystals over 900 μm were observed in the mixture of sample 7 + 8, which is the final sampling. The movement of peak to the right side on x-axis is shown in Fig. 5. It indicates that crystals grow into the bigger crystals as time passed. When excess of supersaturation was reached by MD process, any other process such as evaporation or solvent removal was not needed for crystallization.

4. Conclusion

As the feed water temperature increased, the mass flux of product solution was higher. Since it had a major influence on the water vapor partial pressure, feed temperature was significantly influenced by both permeate flux. Although the permeate flux was directly proportional to temperature difference, the highest rejection (%) was observed at 60˚C. When the test unit was performed at 60˚C, it can ensure more efficient operation with optimum operation conditions of MDC systems. Moreover, MD can concentrate salt solutions in feed reservoir and contribute to make the supersaturated condition in which crystal can grow.

Salt solution including inorganic salt such as $CaSO_4$ can form scale on the membrane, which formation makes the flux decline. The result from this study and others allow us to conclude that two pathways for crystallization were identified: surface crystallization and bulk crystallization. We will conduct further study to determine the relative size of crystallization mechanism depending on various operating conditions such as membrane material and flow velocity.

Acknowledgment

This research was supported by a grant from a Strategic Research Project (Water Reuse Technology for Smart Water Micro-Grids, Code # 2012-0016-1-1) funded by the Korea Institute of Construction Technology.

References

[1] J. Kolodziejski, C. Gasson, Water Reuse Markets 2005–2015: A Global Assessment and Forecast Global Water Intelligence, June, 2005.
[2] G.K. Pearce, UF/MF pre-treatment to RO in seawater and wastewater reuse applications: A comparison of energy costs 222 (2008) 66–73.
[3] Jean-Pierre Mericq, Stephanie Laborie, Corinne Cabassud, Vacuum membrane distillation of seawater reverse osmosis brines, Water Research 44 (2010) 5260–5273.
[4] American Water Works Association, Reverse Osmosis and Nanofiltration, AWWA Manual M46, 2nd ed., 2007.
[5] Sulaiman Al-Obaidani, Efrem Curcio, Potential of membrane distillation in seawater desalination: Thermal efficiency, sensitivity study and cost estimation, Journal of Membrane Science 323 (2008) 85–98.
[6] M.S. El-Bourawi, Z. Ding, R. Ma, M. Khayet, A framework for better understanding membrane distillation separation process, Journal of Membrane Science 285 (2006) 4–29.
[7] Sangho Lee, Jaehong Kim, Chung-Hak Lee, Analysis of $CaSO_4$ scale formation mechanism in various nanofiltration modules, Journal of Membrane Science 163 (1999) 63–74.